Alignment and ordering mechanisms at a liquid crystal-solid interface

G. P. Crawford[a]; R. J. Ondris-Crawford[a]; S. Žumer[ab]; S. Keast[a]; M. Neubert[a]; J. W. Doane[a]

[a] Liquid Crystal Institute, Kent State University, Kent, Ohio, U.S.A. [b] Department of Physics, University of Ljubljana, Ljubljana, Slovenia

PLEASE SCROLL DOWN FOR ARTICLE

Alignment and ordering mechanisms at a liquid crystal–solid interface

By G. P. CRAWFORD*, R. J. ONDRIS-CRAWFORD, S. ŽUMER†,
S. KEAST, M. NEUBERT and J. W. DOANE

Liquid Crystal Institute, Kent State University, Kent, Ohio 44242-0001, U.S.A.

The role of surface coupling agents on the aligning and ordering mechanisms at
a liquid crystal–solid interface are examined with deuterium nuclear magnetic
resonance. The cylindrical channels of alumina membranes 0·2 μm in diameter are
chemically modified using an aliphatic acid ($C_nH_{2n+1}COOH$) as a surface coupling
agent and filled with the liquid crystal compound 4'-pentyl-4-cyanobiphenyl
deuteriated in the α position of the hydrocarbon chain ($5CB-\alpha d_2$). The preferred
anchoring direction at the cavity wall and its strength are found to depend on the
length of the aliphatic chain of the surface coupling agent which determine the
nematic director field in the pores. The planar polar configuration with
homeotropic anchoring conditions is stable for agents with $n \geqslant 7$ while chain lengths
$n \leqslant 6$ support a uniform axial configuration with planar anchoring at the cavity wall.
The pretransitional orientational ordering at the cavity wall above the clearing
temperature is strongly reflected in the spectra. The radical changes in the
quadrupole splitting as the length of the aliphatic chain of the surface coupling agent
is varied indicates strong coupling between the 5CB molecules and the $n = 15$
surface, while shorter chain lengths reveal substantially reduced degrees of coupling.

1. Introduction

In recent years a substantial amount of research has been devoted to understanding
the anchoring and ordering mechanisms of liquid crystal molecules near solid surfaces
[1]. The main reason for the basic interest in surface phenomena of nematic liquid
crystals is that they represent simple examples of complex systems where orientational
wetting, wetting transitions, anchoring transitions, ordering in microconfined systems,
etc., are possible. The principle driving force behind many of the anchoring and related
surface studies is the liquid crystal display. Surface preparation and controlled
alignment play a critical role in the fabrication process of many liquid crystal devices
that depend on uniform orientation of liquid crystal molecules over macroscopic
distances.

The interaction of a liquid crystalline compound with a solid surface depends on the
nature of both the surface and liquid crystal material. In order to obtain a uniform
nematic director pattern between planar glass substrates, the glass is usually modified
with a surface agent that couples the liquid crystal molecules to the glass. Once the
surface coupling agent is applied to the substrate in a careful manner, a specific
orientation of the liquid molecules will be transmitted through the bulk via
intermolecular forces that are responsible for the liquid crystal phase itself. Two
extreme anchoring directions at the solid substrate, namely homeotropic anchoring
where the director assumes an orientation perpendicular to the solid substrates and

---

* Author for correspondence.
    † Permanent address: Department of Physics, University of Ljubljana, Jandranska 19, 61000
Ljubljana, Slovenia

unidirectional planar anchoring where the director is everywhere parallel to one direction in the plane of the substrate, have been extensively studied [2] because of their importance in electrooptical devices.

Homeotropic anchoring can be achieved by depositing soaps or lipids on glass substrates in the following manner. The polar heads of these molecules attach to the glass with the aliphatic chains orthogonal to the interface. Evaporating Au or SiO at oblique incidence on a glass substrate enables liquid crystal molecules to orient along a single planar direction or at an angle to the interface [3, 4]. The most common way to achieve unidirectional planar alignment is to mechanically rub a polyimide treated substrate. The same applies to diamond polished surfaces.

One way to characterize the solid–liquid crystal interaction is to measure the coupling constant that is associated with the interaction. Rapini and Popular [5] first proposed the free energy density associated with the interaction to be of the form

$$f_s = \tfrac{1}{2} W \sin^2 \theta',$$

where θ' is the angle between the preferred and actual anchoring direction. The coupling constant W (anchoring strength) measures the ease at which the orientation can deviate away from its preferred anchoring direction. In general all directions of deviations are not equivalent so the director orientation at the surface is usually described in terms of the polar and azimuthal angles, θ' and φ', respectively. Both principle directions are associated with an anchoring strength, W_θ (polar) and W_φ (azimuthal). Many measurements have been performed on the magnitude of W_θ ranging between 10^{-6}–$10^{-3} \, \mathrm{J} \, \mathrm{m}^{-2}$ and values of W_φ are expected to be one or two orders of magnitude weaker [6–10].

One of the most intriguing aspects of studying the liquid crystal–solid interface is the possibility of an anchoring transition [11]. Ryschenkow and Kleman [12] observed the first anchoring transition; a continuous transition where anchoring characterized by one direction transformed into anchoring characterized by an infinite number of anchoring directions making a fixed angle with respect to the substrate normal as a function of temperature. Hiltrop and Stegemeyer [13] reported similar observations using surfactant monolayers applied to glass substrates. Anchoring transitions were also reported to occur on cleaved mica and gypsum [14] that were driven by the composition of the environment above the nematic cell. Kitzerow *et al.* [14] have induced an anchoring transition by mechanically deforming their muscovite mica surface. Flatischler *et al.* [15] observed a temperature induced abrupt transition from homeotropic-to-planar on lecithin covered surfaces.

The decisive work of Porte [16] demonstrated that the anchoring angle could be varied away from its preferred homeotropic anchoring direction by varying the length of the aliphatic chain of the surface coupling agent ($C_n H_{2n+1}$–NH_2). Porte observed that $n \geqslant 12$ supported homeotropic alignment at the glass substrate and $n \leqslant 10$ gave way to a tilt angle with respect to the preferred homeotropic anchoring direction. The tilt angle was found to increase as the aliphatic chain length decreased. This was one of the initial studies of anchoring phenomena that produced systematic results.

An in depth understanding of the liquid crystal–solid interface requires surface sensitive techniques that are capable of extracting basic parameters which characterize these elusive interactions. Second harmonic generation [17] and small angle X-ray reflectivity [18] measurements are complementary techniques that provide important information about orientational and positional order at the interface, respectively. Evanescent wave ellipsometry [19] is another proficient technique to extract

information on the orientational order parameter at the surface. Scanning tunnelling microscopy allows an image of the molecules at the substrate boundary [20]. In the past few years there has been a great deal of interest in confining liquid crystals to microporous membranes and to well-defined geometries. The large surface to volume ratio of these systems allows techniques such as nuclear magnetic resonance [21], dielectric spectroscopy [22] and heat capacity [23] to probe surface interactions. These confining systems include porous glass [24], porous polycarbonate membranes [25], porous alumina membranes [26], gel systems [27] and polymer dispersed liquid crystal (PDLC) materials [28].

The pioneering work of Golemme [21] revealed that deuterium nuclear magnetic resonance (^{2}H NMR) could be used as a tool to identify the nematic director field configurations in submicrometer spherical cavities. Golemme [29] further demonstrated that the weakly first order nematic–isotropic transition evolves into a continuous change from paranematic to nematic order in a limiting cavity size. This was the first experiment to confirm the theoretical predictions of Sheng [30]. Subsequent magnetic resonance studies by Vilfan and co-workers [31] provided evidence that the local molecular reorientations of the liquid crystal molecules at the surface of the spherical cavity are hindered.

Recently, it was discovered that a detailed analysis of the stable nematic director configurations in cylindrically shaped cavities could provide information on molecular anchoring and surface elastic properties [32]. The cylindrical cavities of Polycarbonate membranes were permeated with a liquid crystal compound. This allows the nematic director distributions inside these cavities to be accurately studied with ^{2}H NMR enabling the average defect density [33], the molecular anchoring angle and strength [34], and the saddle-splay surface elastic constant K_{24} [32, 34] to be determined. These studies were followed up by theoretical treatments of defect–defect interactions in cylindrical containers by Vilfan *et al.* [35]. The initial experiments on Nuclepore membranes demonstrating the feasibility of cylindrical containment of liquid crystals were introduced by Kuzma and Labes [36] who investigated the role of increased curvature on the nematic–isotropic transition temperatures.

^{2}H NMR of liquid crystals confined to porous polycarbonate [37] and porous alumina [38] membranes Anopore above the clearing temperature first disclosed evidence for a weakly orientationally ordered nematic-like layer well above the transition temperature. The translational diffusion properties in this layer were found to be dramatically different from the bulk material. The temperature dependence of the surface order parameter in these systems was shown to strongly depend on the preparation of the confining substrate. Heat capacity measurements [23, 39] of liquid crystals confined to Anopore membranes revealed a radically different behaviour at the nematic–isotropic transition depending on the orientation of the liquid crystal molecules in the cavities and the order of the transition. Other studies on interfacial interactions include small angle X-ray and dielectric spectroscopy [22] on porous glass filled with liquid crystals. ^{2}H NMR studies on the interaction of liquid crystal molecules with a fragile polymer network (sometimes referred to as gel) provide information on the orientation and order of such systems [27].

The generic orienting mechanisms that govern the interactions occurring at a liquid crystal–solid interface can be classified into two categories: short range substrate–fluid anisotropic interactions generally chemical in nature and long range fluid–fluid interactions that are responsible for the liquid crystalline properties. Several theories based on Landau–de-Gennes formalism [40–44], Maier–Saupe [45] and molecular

approaches [46] have been developed to describe orientational ordering near a solid surface. The value of the orientational order parameter at the surface is a direct measure of the anisotropic substrate–fluid potential. Many interesting types of surface phenomena are predicted to occur depending on the strength of the surface coupling constant, such as wetting and prewetting transitions [40, 41, 45], surface melting [47], and the possibility of a symmetry breaking transition [48].

Our ^{2}H NMR studies on the liquid crystal–solid interaction using confining techniques to obtain a large surface to volume ratio have progressed rapidly over the past 2 years. We are now in a position to present studies on confined liquid crystals where the interaction at the interface is systematically controlled. In this contribution, we present a study of the liquid crystal–solid interaction which is controlled by varying the surface coupling agent used to obtain a preferential alignment. The cylindrical channels of Anopore membranes (see figure 1) are chemically modified with an aliphatic acid $(C_nH_{2n+1}COOH)$, where the effects of the aliphatic chain length on the anchoring direction and orientational order parameter at the surface are studied. The acid head group strongly adheres to the alumina surface with the aliphatic chain pointing along the surface normal. A wide range of chain lengths were used, $5 \leqslant n \leqslant 15$, which enable the effect of the aliphatic chain on the ordering mechanisms at the surface to be studied. The carbon number n is found to strongly affect the nematic director field configuration, and the degree of orientational order at the surface above the nematic–isotropic transition temperature.

2. Materials

The cylindrical channels of Anopore membranes (see figure 1) filled with the liquid crystal compound 5CB-αd_2 provide an ideal system to probe molecular interactions occurring near solid surfaces using ^{2}H NMR [26]. The membrane is composed of a high purity alumina matrix with $0.2\,\mu m$ diameter cylindrical channels that penetrate

Membrane
Surface

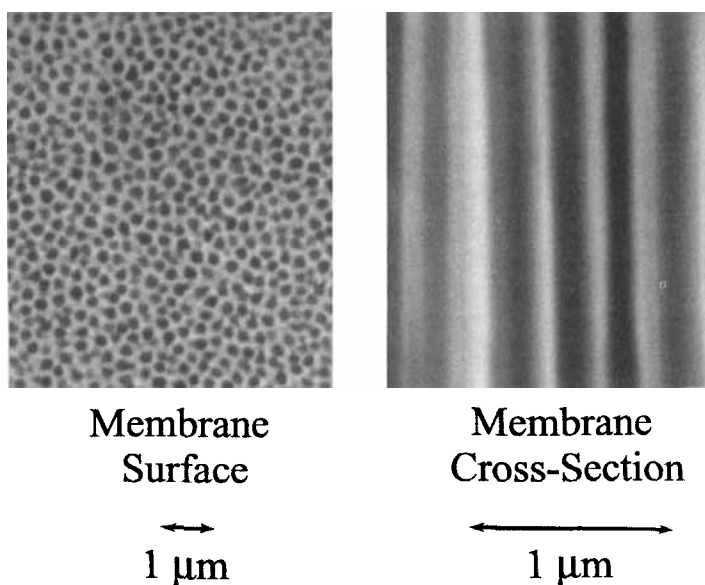Membrane
Cross-Section

1 μm   1 μm

Figure 1.   Scanning electron microscope photograph of the surface of an Anopore membrane. The rated pore diameter of the cylindrical channels is $0.2\,\mu m$.
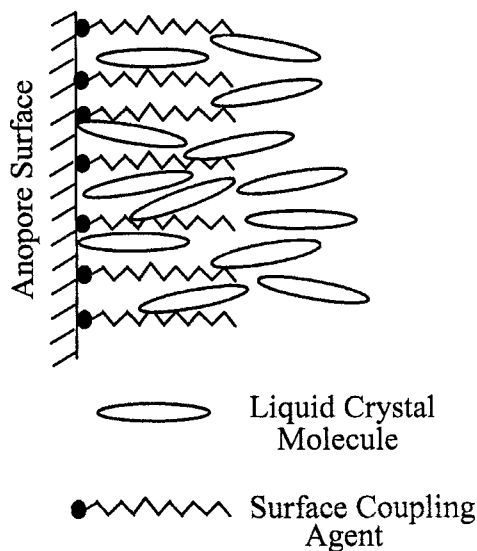
Figure 2. Illustration of homeotropic alignment occurring at the cavity wall of the alumina Anopore membrane. The aliphatic acid is used to couple the alumina surface to the liquid crystal.

through its 60 μm thickness [49]. The membranes are treated with a 2 per cent by weight solution of an aliphatic acid ($C_nH_{2n+1}COOH$) in methanol and quickly placed in a vacuum oven for approximately 1 hour. The acid head group chemically bonds to the surface and the aliphatic chains form a compact assemblage perpendicular to the cavity wall. The liquid crystal is introduced into the membranes and heated to the isotropic phase for several hours to ensure a complete fill. The polar head group of the aliphatic acid interacts with the solid surface and the aliphatic chain couples the liquid crystal to the surface (see figure 2). Several samples were prepared by varying the carbon number, n, of the aliphatic acid coupling agent using the same liquid crystal compound 5CB-αd_2.

3. Experimental

^{2}H NMR is a powerful tool to probe the orientational order parameter in confined geometries. It has also been used to accurately identify the nematic director fields that occur in spherical [21] and cylindrical geometries [33], and the anchoring direction of the elongated liquid crystal molecules at the cavity surface [32, 34]. Its success can be traced to its ability to extract the orientation and order parameter of the liquid crystal directly from the quadrupole frequency given by

$$\delta v = \pm \frac{S(r)}{S_B} \delta v_B \left(\frac{3}{2} \cos^2 \theta(\mathbf{r}) - \frac{1}{2} \right), \tag{1}$$

where $\theta(\mathbf{r})$ is the angle between the local nematic director and the magnetic field, $S(r)$ is the local order parameter, and $\delta v_B/S_B$ is the ratio between the quadrupole splitting frequency and the order parameter of the bulk nematic. The influence of motional averaging is presented in §4 for the nematic and isotropic phases.

The orienting effect of the magnetic field, **B**, of the NMR spectrometer on the nematic liquid crystal depends on the anisotropy in diamagnetic susceptibility, $\Delta\chi$, and the elastic constant, K, of the nematic material. The influence of the magnetic field can be estimated by calculating the magnetic coherence length ξ_m, given by

$$\xi_m = \left(\frac{\mu_0 K}{\Delta\chi}\right)^{1/2} \frac{1}{B}. \tag{2}$$

The magnetic field strength of our NMR spectrometer is 4·7 T which corresponds to a magnetic coherence length of $\xi_m = 1·7\,\mu m$. This is substantially larger than the cavity sizes employed in this study and exceeds the thickness of the surface induced nematic order above the clearing temperature by several orders of magnitude. Therefore the magnetic field will not introduce any measurable distortion in our studies.

4. Results and discussion

The specific nematic director field configuration in a cylindrical environment depends on the interplay between elastic forces of the nematic material, the effects of external fields, the morphology and size of cavity and the strength of the interactions occurring at the cavity wall. The specific functional form of the director field can be predicted from elastic theory [32, 34, 50]

$$F = \frac{1}{2}\int_V \{K_{11}(\nabla\cdot\mathbf{n})^2 + K_{22}(\mathbf{n}\cdot\nabla\times\mathbf{n})^2 + K_{33}(\mathbf{n}\times\nabla\times\mathbf{n})^2$$

$$- K_{24}(\mathbf{n}\times\nabla\times\mathbf{n} + \mathbf{n}\nabla\cdot\mathbf{n})\}\,dV$$

$$- \frac{1}{2}\int_V \frac{\Delta\chi}{\mu_0}(\mathbf{B}\cdot\mathbf{n})^2 dV + \frac{1}{2}\int_S W_0 \sin^2(\theta' - \theta'_0)\,dA, \tag{3}$$

where K_{11}, K_{22} and K_{33} are the traditional splay, twist and bend bulk elastic constants, respectively, and K_{24} is the saddle splay surface elastic constant. The final term is the anisotropic part in the surface free energy; W_0 is the molecular anchoring strength and θ' and θ'_0 are the preferred and actual anchoring angles, respectively. The nematic director patterns for cylindrical environments have been worked out in detail [33, 34] so they will not be discussed here. The ^{2}H NMR patterns will be compared to simulated spectral patterns calculated using predictions of equation (3).

If we consider a truly isotropic liquid crystal sample, there is no quadrupole interaction resulting in a single absorption line. However, since Anopore systems exhibit a large surface to volume ratio, the presence of the surface introduces some orientational order into the system. ^{2}H NMR is sensitive to this small degree of surface induced orientational order and can measure the order parameter at the surface [37, 38]. The approximate profile to describe surface induced order is given by the expression [19]

$$S(r) = S_0 \exp[-(R - r)/\xi], \tag{4}$$

where S_0 is the order parameter at the cavity wall, R is the radius of the capillary and $\xi = \xi_0 [(T - T^*)/T^*]^{-1/2}$, ξ_0 is the zero temperature correlation length determined to be 0·65 nm for 5CB [51], and T^* is the supercooling limit temperature which is 1·1 K below the bulk nematic–isotropic transition temperature [51]. Equation (4) is derived for $S_0 \ll 1$ by neglecting higher order terms and neglecting the effect of confinement ($\xi \ll R$) [52].

4.1. *Nematic phase*

The effect of translational self-diffusion on NMR signals in the nematic phase can be estimated by comparing the range that the molecule diffuses on the NMR time scale, $x \sim \sqrt{(D/\delta v)}$, to the distance where the director changes appreciably. Using typical values of the diffusion constant, $D = 10^{-11} \, \mathrm{m^2 \, s^{-1}}$, and the quadrupole splitting of the macroscopically aligned bulk, $\delta v_B = 40 \, \mathrm{kHz}$, the range the molecule diffuses is $x = 0.02 \, \mu\mathrm{m}$, which is an order of magnitude smaller than the cavity sizes employed in this study. Therefore we expect that the effects from diffusion are negligible which results in a $^2\mathrm{H}$ NMR spectral pattern that reflects a static distribution of directors in the cylinder.

The $^2\mathrm{H}$ NMR spectral patterns of 5CB-αd_2 confined in the $0.2 \, \mu\mathrm{m}$ treated cavities of Anopore membranes are presented in figure 3. The spectra are recorded at room temperature ($11°\mathrm{C}$ below the clearing temperature) for a variety of carbon numbers, n, associated with the aliphatic acid surface coupling agent. For a more precise structure determination two orientations of the cylindrical axis in the magnetic field are recorded: $\theta_B = 0°$ corresponds to the cylindrical axis being parallel to the magnetic field and $\theta_B = 90°$ corresponds to the cylindrical axis being perpendicular to the magnetic field. The $^2\mathrm{H}$ NMR spectral patterns reveal an abrupt configuration change when $n = 6$. For $n \geqslant 7$, the spectra are interpreted as the planar polar configuration (see figure 4) where the symmetry axes of the configuration remain randomly oriented in the magnetic field. When $\theta_B = 0°$ two absorption lines are observed separated by a quadrupole splitting frequency of $\frac{1}{2}\delta v_B$ which is characteristic of any planar configuration. Unfortunately, no anchoring strength information can be obtained since the $\theta_B = 0°$ orientation is insensitive to the anchoring angle and the random alignment of the symmetry axes of the planar polar configuration with respect to **B** in the $\theta_B = 90°$ orientation does not allow for a direct measurement of the anchoring strength. A planar radial configuration (see figure 4) would also be consistent with the spectra in $\theta_B = 90°$ ($n \geqslant 7$) in figure 3, but free energy considerations reveal that the planar polar configuration is energetically favourable when K_{11} and K_{33} are comparable [34]. In fact, the planar radial configuration is not expected until $K_{33} \gg K_{11}$ [53].

For $n \leqslant 6$, the spectral patterns are radically different revealing that a configurational change has occurred as a function of chain length of the surfactant molecule used as the surface coupling agent. The new configuration is a uniform axial structure (no elastic deformation) with planar anchoring conditions (see figure 4). A discrete change in the configuration and the anchoring direction at the cavity wall has occurred at a critical length of the aliphatic chain of the surface coupling agent. According to our interpretation, the chain length of the coupling agent decreases which results in the anchoring strength associated with the polar (out of plane) component to effectively weaken until it no longer can support homeotropic alignment. This is consistent with earlier treatments on sterical hindrance [54–56]. At this point the anchoring abruptly changes to a planar anchoring which supports the axial director configuration.

4.2. *Isotropic phase*

When these systems are taken into the isotropic phase, a partial nematic order still exists in regions near the surface that can be described by equation (4). The presence of orientational order is responsible for the definite quadrupole splitting frequency observed in the isotropic phase (see figure 3). The effects of diffusion are dramatically different in the isotropic phase as compared to the nematic phase. The characteristic length of diffusion, $x \sim \sqrt{(D/\delta v)}$, is approximately $0.3 \, \mu\mathrm{m}$ which is larger than our pore
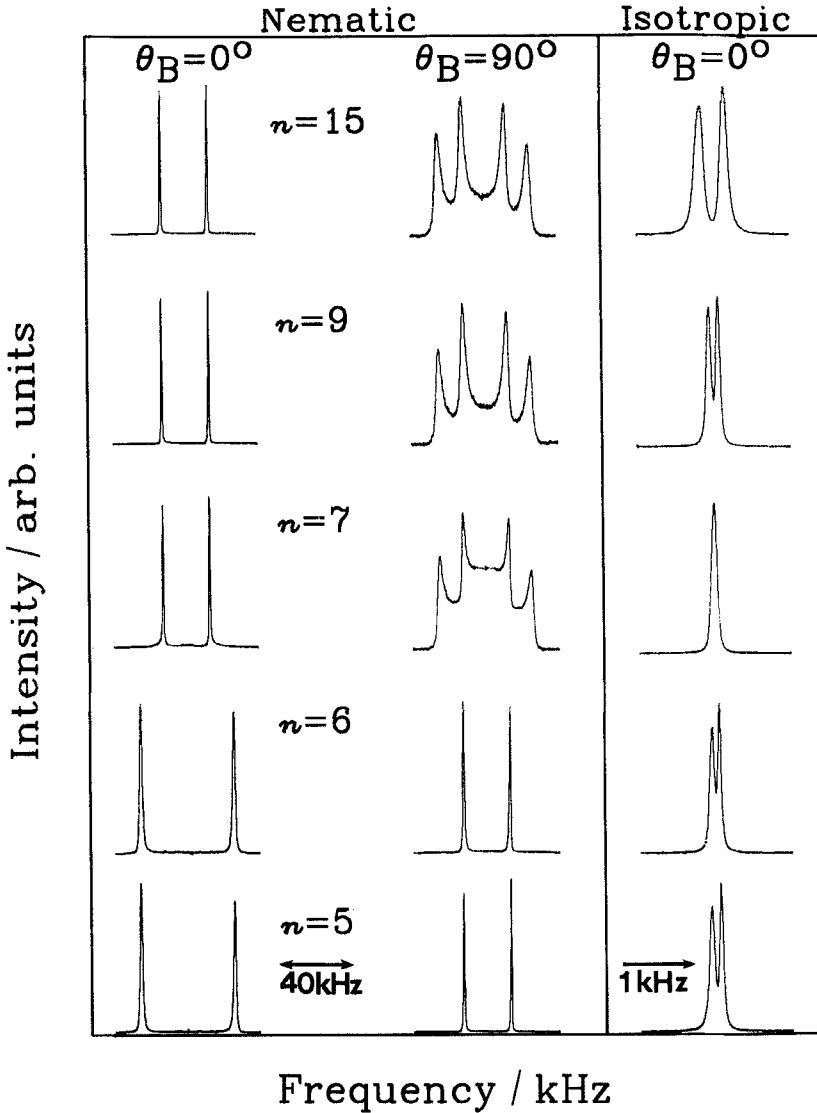
Figure 3. Deuterium NMR spectral patterns of 5CB-αd_2 confined to the treated cavities of Ancpore membranes. The alumina cavities of the membrane are coupled to the liquid crystal with the aliphatic acid C_nH_{2n+1}–COOH where the length of the aliphatic chain, n, is varied. The spectra accumulated in the nematic phase were recorded at 24°C for two orientations of the cylindrical axis in the magnetic field. The spectra accumulated in the isotropic phase were recorded at 37°C with the cylindrical axis parallel to the magnetic field.
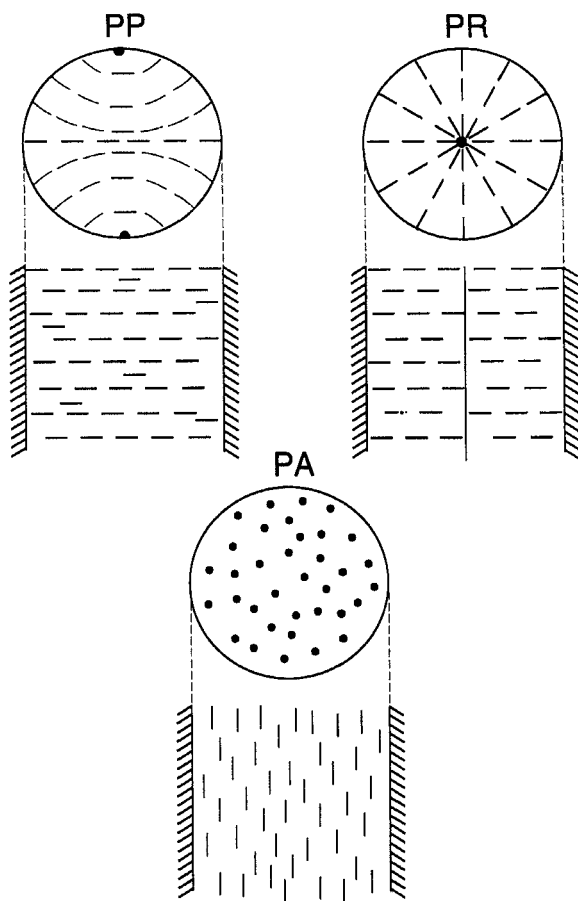
Figure 4. Three possible nematic director configurations that occur in cyclindrical cavities: The planar polar (PP) and planar radial (PR) require homeotropic anchoring at the cavity wall and the uniform parallel axial (PA) structure has homogeneous anchoring conditions.

diameter and much larger than the thickness of the ordered surface layer which is usually about 2 nm. Therefore a diffusing molecule samples the order throughout the cross section of the cavity (fast motional averaging). The small cavity size and the long time scale of the NMR measurement in the isotropic phase (milliseconds) allows us to simplify our analysis.

The ^{2}H NMR spectra, recorded at 2·5°C above the nematic–isotropic transition, are presented in figure 3 for various lengths of the aliphatic chain of the surface coupling agent. The averaged quadrupole splitting frequency $\langle \delta v \rangle$ is linearly related to S_0 [38]. A very interesting evolution of the spectra takes place as n is decreased. The larger splitting in the $n = 15$ case indicates rather strong coupling at the surface. As the aliphatic chain length is decreased, the coupling with the surface decreases until $n = 7$ where there is no measurable quadrupole splitting. The quadrupole splitting becomes resolvable at $n = 6$ again and is found to increase at $n = 5$. This very interesting behaviour suggests that besides the modification of the anchoring direction, the orientational order parameter at the surface can also be controlled by varying the length of the aliphatic chain of the surface coupling agent.

G. P. Crawford *et al.*
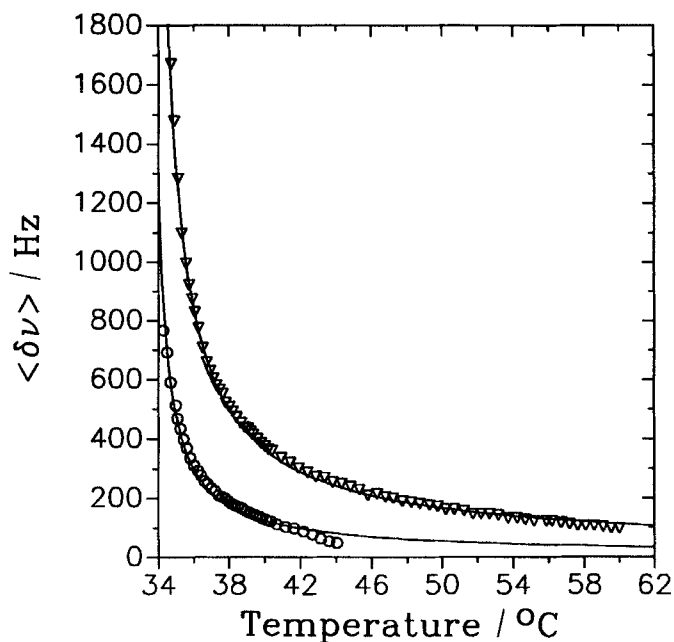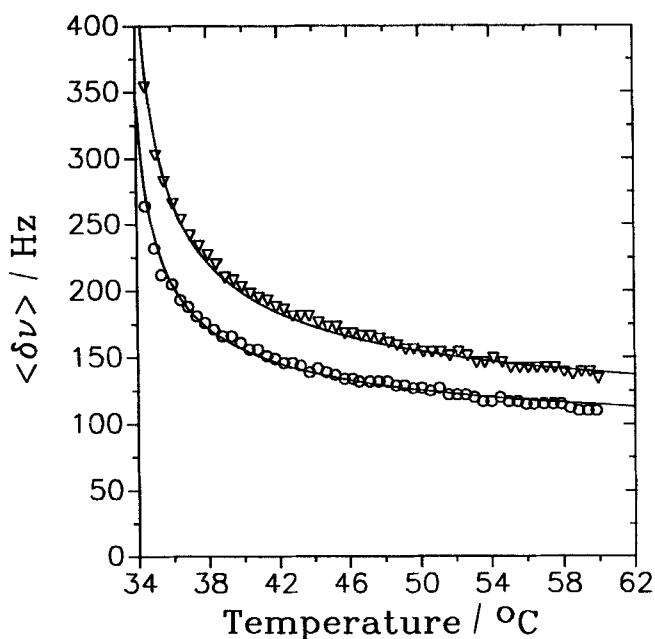
Figure 5. The average quadrupole splitting $\langle \delta v \rangle$ as a function of temperature approaching the nematic–isotropic transition temperature from above for perpendicular (*a*) and parallel (*b*) anchoring conditions. The solid line denotes the theoretical fit where the fitted interfacial parameters are presented in the table. For $n = 15$ and 9, S_0 is found to be temperature dependent according to $S_0 \propto (T - T^*)^{-1/2}$ with $S_0(T - T^* = 0.4 \, \text{K})$ given in the table. For $n = 6$ and 5, S_0 is found to be constant over the entire temperature range with values of S_0 presented in the table. (*a*) ∇, $C_{15}H_{31}$–COOH; $\bigcirc$, C_9H_{19}–COOH. (*b*) ∇, C_5H_{11}–COOH; $\bigcirc$, C_6H_{13}–COOH.

Summary of interfacial parameters measured from NMR spectra. The cylindrical pores of Anopore membranes were chemically modified with the surface coupling agent C_nH_{2n+1}–COOH and filled with 5CB-αd_2. A 2 by weight solution of C_nH_{2n+1}–COOH in methanol was used.

Chain length n	Anchoring[†]	$S_0(T-T_{NI}=0{\cdot}4\,\text{K})$	l_0 nm
15	Homeotropic	$0{\cdot}13 \pm 0{\cdot}02$	$1{\cdot}5 \pm 0{\cdot}5$
9	Homeotropic	$0{\cdot}05 \pm 0{\cdot}01$	$0{\cdot}8 \pm 0{\cdot}5$
7	Homeotropic	—	—
6	Planar	$0{\cdot}01 \pm 0{\cdot}005$[‡]	$2{\cdot}5 \pm 1{\cdot}0$
5	Planar	$0{\cdot}01 \pm 0{\cdot}005$[‡]	$2{\cdot}0 \pm 1{\cdot}0$

† Anchoring direction confirmed in nematic phase.
‡ The value of S_0 is the same over the entire temperature range studied.

The temperature dependence of the average quadrupole splitting frequency for the various surface preparations is presented in figure 5. One important point about the sensitivity of the NMR technique is its ability to detect surface induced order deep into the isotropic phase. It was previously shown that the traditional theoretical approaches could not describe the amount of order measured far away from the nematic–isotropic transition [37, 38] where order occurs in a layer thickness comparable to the molecular length. The data could be more accurately analysed by including a molecular layer at the surface of thickness, l_0, where the value of the orientational order S_0 persists, while on distances larger than l_0 its penetration into the cavity follows the form of equation (3). Further evidence of a different behaviour in the first molecular layer is the molecular exchange rate between the surface layer and the bulk which is substantially different than the estimated exchange rate if bulk diffusion constant values were used. We follow this same analysis [37, 38] in our preliminary determination of S_0 and l_0.

The analysis of our NMR data presented in figure 5 is summarized in the table. The data presented in the table clearly demonstrate the delicate dependence of the liquid crystal molecules with the coupling agent at the solid surface. The order parameter of the liquid crystal molecules at the surface is extremely sensitive to the length of the aliphatic chain of the surface coupling constant. Furthermore, the temperature dependence of S_0 is also affected by the length of the aliphatic chain of the coupling agent. For $n = 15$ and 9, $S_0(T)$ shows a strong increase on approaching the nematic–isotropic transition temperature from above which approximately follows the functional form derived by Sheng [41],

$$S_0 = G/\sqrt{(4aL(T - T^*))}$$

where G is the surface coupling constant in units $J\,m^{-2}$, a is the Landau–de-Gennes expansion coefficient, and L is the elastic constant [51]. For $n = 6$ and 5, S_0 is non-critical and remains constant over the entire temperature range studied. Our observations show that systems that exhibit parallel anchoring conditions give way to weaker surface order parameters and non-critical temperature dependences of the surface order parameter corresponding to partial nematic wetting. More studies are underway to complete the picture on pretransitional ordering and nematic wetting [57].

5. Conclusions

We have presented conclusive evidence that the ordering and anchoring mechanisms in confined geometries can be systematically controlled by varying the length of the aliphatic chain of the surface coupling agent. Deuterium NMR is used as a sensitive method to detect nematic ordering in the porous systems. A configurational transition is reported to occur from the planar polar structure to the uniform axial structure indicating a discrete transition from homeotropic to planar anchoring as the aliphatic chain length on the surfactant molecule is changed from $n = 7$ to $n = 6$. This indicates that the preferred anchoring direction has discontinuously changed from normal to planar at the surface. Radical differences in the quadrupole splitting frequency are also observed above the nematic–isotropic transition revealing the sensitivity of the surface coupling agent on the nematic ordering mechanisms in the vicinity of the cavity wall. Further studies are planned to complete the picture of surface induced orientational ordering, symmetry breaking transitions, nematic wetting transitions, etc., in these systems [57].

References

[1] JÉRÔME, B., 1991, *Rep. Prog. Phys.*, **54**, 391 and references therein.
[2] COGNARD, J., 1982, *Molec. Crystals liq. Crystals Suppl.*, **1**, 1 and references therein.
[3] DE JEU, W. H., 1980, *Physical Properties of Liquid Crystalline Materials* (Gordon & Breach Science Publishers), Chap. 2.
[4] KLEMAN, M., 1983, *Points, Lines and Walls: in Liquid Crystals, Magnetic Systems and Various Ordered Media* (Wiley, New York), Chap. 3.
[5] RAPINI, A., and PAPOULAR, M., 1969, *J. Phys., Paris, Colloq.*, **30**, C4-54.
[6] RIVIERE, D., LEVY, Y., and GUYON, E., 1979, *J. Phys. Lett., Paris*, **40**, L-215.
[7] YOKOYAMA, H., and VAN SPRANG, H. A., 1985, *J. appl. Phys.*, **57**, 4520.
[8] YOKOYAMA, H., KOBAYENKOV, S., and KAMEI, H., 1987, *J. appl. Phys.*, **61**, 4501.
[9] BLINOV, L. M., YU, A., and SONIN, A. A., 1989, *Liq. Crystals*, **5**, 645.
[10] ERDMANN, J. H., ŽUMER, S., and DOANE, J. W., 1990, *Phys. Rev. Lett.*, **64**, 1907.
[11] PIERANSKI, P., and JÉRÔME, B., 1991, *Molec. Crystals liq. Crystals*, **199**, [645]/167.
[12] RYSCHENKOW, G., and KLEMAN, M., 1976, *J. chem. Phys.*, **64**, 404.
[13] HILTROP, K., and STEGEMEYER, H., 1981, *Bunsenges phys. Chem.*, **85**, 582.
[14] PIERANSKI, P., and JÉRÔME, B., 1989, *Phys. Rev. A*, **43**, 317; BECHHOEFER, J., DUVAIL, J. L., MASSON, L., JÉRÔME, B., HORNREICH, R. M., and PIERANSKI, P., 1990, *Phys. Rev. Lett.*, **64**, 1911. KITZEROW, H. S., JÉRÔME, B., and PIERANSKI, P., 1991, *Physica A*, **174**, 163.
[15] FLATSICHLER, K., KOMITOV, L., LAGERWALL, S. T., STEBLER, B., and STRIGAZZI, A., 1991, *Molec. Crystals liq. Crystals*, **198**, 119.
[16] PORTE, G., 1976, *J. Phys. Paris*, **10**, 1245.
[17] SHEN, Y. R., 1988, *Nature, Lond.*, **337**, 519 and references therein.
[18] ALS-NIELSEN, J., 1987, *Topics in Current Physics*, Vol. 43, edited by W. Schommers and P. van Blackenhagen (Springer).
[19] CHEN, W., MARTINEZ-MIRANDA, L. J., HSIUNG, H., and SHEN, Y. R., 1990, *Molec. Crystals liq. Crystals*, **179**, 419; 1989, *Phys. Rev. Lett.*, **62**, 1860. GUYOT-SIONNEST, P., HSIUNG, H., and SHEN, Y. R., 1986, *Phys. Rev. Lett.*, **57**, 2963.
[20] SMITH, D., HORBER, H., GERBER, C., and BINNIG, G., 1989, *Science, N.Y.*, **245**, 43. FOSTER, J. S., and FROMMER, J. E., 1988, *Nature, Lond.*, **333**, 542.
[21] GOLEMME, A., ŽUMER, S., DOANE, J. W., and NEUBERT, M., 1988, *Phys. Rev. A*, **37**, 559.
[22] ALIEV, F. M., and BREGANOV, N., 1989, *Sov. Phys. J.E.T.P.*, **68**, 70 [1989, *Zh. eksp. teor. Fiz.*, **95**, 122)].

[23] IANNACCHIONE, G. I., CRAWFORD, G. P., DOANE, J. W., and FINOTELLO, D., 1992, *Molec. Crystals liq. Crystals*, **222**, 205.
[24] LEVITZ, P., EHRET, G., SINHA, S. K., and DRAKE, J. M., 1991, *J. chem. Phys.*, **95**, 6151.
[25] MOORE, J. C., 1969, *The Development of a New Membrane Filter* (American Laboratory).
[26] HOFFMANN, J., 1989, *Am. Lab.*, **21**, 70.
[27] STANNARIUS, R., CRAWFORD, G. P., CHIEN, L. C., and DOANE, J. W., 1991, *J. appl. Phys.*, **70**, 135; BELLINI, T., CLARK, N. A., MUZNY, C. D., WU, L., GARLAND, C. W., SCHAEFER, D. W., and OLIVER, B. J., 1992, *Phys. Rev. Lett.*, **69**, 788.
[28] DOANE, J. W., 1990, *Liquid Crystals: Applications and Uses*, edited by B. Bahadur (World Scientific), Chap. 14.
[29] GOLEMME, A., ŽUMER, S., ALLENDER, D. W., and DOANE, J. W., 1988, *Phys. Rev. Lett.*, **61**, 1937.
[30] SHENG, P., 1982, *Phys. Rev. A*, **26**, 1610.
[31] VILFAN, M., RUTAR, V., ŽUMER, S., LAHAJNAR, G., BLINC, R., DOANE, J. W., and GOLEMME, A., 1988, *J. Chem. Phys.*, **89**, 579. DOLINŠEK, J., JARH, O., VILFAN, M., ŽUMER, S., BLINC, R., DOANE, J. W., and CRAWFORD, G., 1991, *J. chem. Phys.*, **95**, 2154.
[32] CRAWFORD, G. P., ALLENDER, D. W., DOANE, J. W., VILFAN, M., and VILFAN, I., 1991, *Phys. Rev. A*, **44**, 2570.
[33] CRAWFORD, G. P., VILFAN, M., VILFAN, I., and DOANE, J. W., 1991, *Phys. Rev. A*, **43**, 835.
[34] ALLENDER, D. W., CRAWFORD, G. P., and DOANE, J. W., 1991, *Phys. Rev. Lett.*, **67**, 1442. CRAWFORD, G. P., 1991, Ph.D Dissertation, Kent State University. CRAWFORD, G. P., ALLENDER, D. W., and DOANE, J. W., 1992, *Phys. Rev. A*, **45**, 8693.
[35] VILFAN, I., VILFAN, M., and ŽUMER, S., 1991, *Phys. Rev. A*, **43**, 6875.
[36] KUZMA, M., and LABES, M. M., 1983, *Molec. Crystals liq. Crystals*, **100**, 103.
[37] CRAWFORD, G. P., YANG, D. K., ŽUMER, S., FINOTELLO, D., and DOANE, J. W., 1991, *Phys. Rev. Lett.*, **66**, 723.
[38] CRAWFORD, G. P., STANNARIUS, R., and DOANE, J. W., 1991, *Phys. Rev. A*, **44**, 2558.
[39] IANNACCHIONE, G. S., and FINOTELLO, D., 1992, *Phys. Rev. Lett.*, **69**, 2094.
[40] DE GENNES, P. G., 1985, *Rev. mod. Phys.*, **57**, 827.
[41] SHENG, P., 1976, *Phys. Rev. Lett.*, **37**, 1059.
[42] ALLENDER, D. W., HENDERSON, G. L., and JOHNSON, D. L., 1981, *Phys. Rev. A*, **24**, 1086.
[43] MAUGER, A., ZRIBI, G., MILLS, D. L., and TONER, J., 1984, *Phys. Rev. Lett.*, **53**, 2485.
[44] SEN, A. K., and SULLIVAN, D. E., 1987, *Phys. Rev. A*, **35**, 1391.
[45] SLUKIN, T. J., and PONIERWIERSKI, A., 1986, *Fluids of Interfacial Phenomena*, edited by C. A. Croxton (Wiley), Chap. 5 and references therein.
[46] TELO DA GAMMA, M. M., 1984, *Molec. Phys.*, **52**, 585; 1984, *Ibid.*, **52**, 611; 1987, *Phys. Rev. Lett.*, **59**, 154.
[47] BARBERI, B., and DURAND, G., 1990, *Phys. Rev. A*, **41**, 2207. BARBERO, G., and DURAND, G., 1991, *J. Phys. II*, **1**, 651.
[48] SLUCKIN, T. J., and PONIEWIERSKI, A., 1985, *Phys. Rev. Lett.*, **55**, 2907. HORNREICH, R. M., KATS, E. I., and LEBEDEV, V. V., 1992, *Phys. Rev. A*, **46**, 4935. SHENG, P., LI, B.-Z., ZHOU, M., MOSES, T., and SHEN, Y. R., 1992, *Phys. Rev. A*, **46**, 946.
[49] CRAWFORD, G. P., STEELE, L. M., ONDRIS-CRAWFORD, R., IANNACCHIONE, S., YEAGER, C. J., DOANE, J. W., and FINNOTELLO, D., 1992, *J. chem. Phys.*, **96**, 7788.
[50] KRALJ, S., and ŽUMER, S., 1992, *Phys. Rev. A.* **45**, 2461; ŽUMER, S., KRALJ, S., and BEZIC, J., 1992, *Molec. Crystals liq. Crystals*, **212**, 163.
[51] COLES, H. J., 1978, *Molec. Crystals liq. Crystals*, **49**, 67.
[52] KRALJ, S., ŽUMER, S., and ALLENDER, D. W., 1991, *Phys. Rev. A*, **43**, 2943.
[53] CLADIS, P. E., 1974, *Phil. Mag.*, **29**, 641.
[54] PROUST, J. E., MINASSIAN-SARAGA, T., and GUYON, L., 1972, *Solid St. Commun.*, **11**, 1227.
[55] CREAGH, L. T., and KMETZ, A. R., 1974, *4th International Liquid Crystal Conference*, Kent, Ohio, U.S.A.
[56] KAHN, F. J., and TAYLOR, B. N., 1973, *Proc. I.E.E.E.*, **61**, 823.
[57] CRAWFORD, G. P., ONDRIS-CRAWFORD, R., ŽUMER, S., and DOANE, J. W., 1993, *Phys. Rev. Lett.*, **70**, 1838.